Published in final edited form as:
Cancer Res. 2010 June 15; 70(12): 4868–4879. doi:10.1158/0008-5472.CAN-09-4404.

Fibroblast Growth Factor Receptor Signaling Dramatically Accelerates Tumorigenesis and Enhances Oncoprotein Translation in the Mouse Mammary Tumor Virus–Wnt-1 Mouse Model of Breast Cancer

Adam C. Pond[1], **Jason I. Herschkowitz**[2], **Kathryn L. Schwertfeger**[6], **Bryan Welm**[7], **Yiqun Zhang**[4], **Brian York**[2], **Robert D. Cardiff**[8], **Susan Hilsenbeck**[3], **Charles M. Perou**[9], **Chad J. Creighton**[4], **Richard E. Lloyd**[5], and **Jeffrey M. Rosen**[2]

[1]Program in Cell and Molecular Biology, Baylor College of Medicine, Houston, Texas

[2]Department of Molecular and Cellular Biology, Baylor College of Medicine, Houston, Texas

[3]Lester and Sue Smith Breast Center, Baylor College of Medicine, Houston, Texas

[4]Dan L. Duncan Cancer Center, Baylor College of Medicine, Houston, Texas

[5]Molecular Virology and Microbiology, Baylor College of Medicine, Houston, Texas

[6]Department of Laboratory Medicine and Pathology and Masonic Cancer Center, University of Minnesota, Minneapolis, Minnesota

[7]Department of Surgery, University of Utah Huntsman Cancer Institute, Salt Lake City, Utah

[8]Department of Medical Pathology and Laboratory Medicine, Center for Comparative Medicine, University of California, Davis, California

[9]Departments of Genetics and of Pathology and Laboratory Medicine, Lineberger Comprehensive Cancer Center, University of North Carolina, Chapel Hill, North Carolina

Abstract

Fibroblast growth factor (FGF) cooperates with the Wnt/β-catenin pathway to promote mammary tumorigenesis. To investigate the mechanisms involved in FGF/Wnt cooperation, we genetically engineered a model of inducible FGF receptor (iFGFR) signaling in the context of the well-established mouse mammary tumor virus–Wnt-1 transgenic mouse. In the bigenic mice, iFGFR1 activation dramatically enhanced mammary tumorigenesis. Expression microarray analysis did not show transcriptional enhancement of Wnt/β-catenin target genes but instead showed a translational gene signature that also correlated with elevated FGFR1 and FGFR2 in human breast cancer data sets. Additionally, iFGFR1 activation enhanced recruitment of RNA to polysomes, resulting in a marked increase in protein expression of several different Wnt/β-catenin target genes. FGF pathway activation stimulated extracellular signal-regulated kinase and the phosphorylation of key translation regulators both *in vivo* in the mouse model and *in vitro* in a human breast cancer cell line. Our results suggest that cooperation of the FGF and Wnt pathways in mammary tumorigenesis is based on the activation of protein translational pathways that result in, but are not

Corresponding Author: Adam C. Pond, Program in Cell and Molecular, Biology, Baylor College of Medicine, One Baylor Plaza, Houston, TX, 77030. Phone: 713-392-8277; Fax: 713-798-8012; apond@bcm.tmc.edu.

Note: Supplementary data for this article are available at Cancer Research Online (http://cancerres.aacrjournals.org/).

Disclosure of Potential Conflicts of Interest
No potential conflicts of interest were disclosed.

limited to, increased expression of Wnt/β-catenin target genes (at the level of protein translation). Further, they reveal protein translation initiation factors as potential therapeutic targets for human breast cancers with alterations in FGF signaling.

Introduction

Despite improvements in diagnosis and treatment, breast cancer remains the second leading cause of cancer death in American women (American Cancer Society, 2007). The development of therapeutics targeting key signaling pathways important in human breast cancer, notably estrogen receptor (ER) and heregulin, has accounted for the recent decrease in mortality of several breast cancer subtypes (1). However, continued improvements in treatment will undoubtedly depend on our ability to identify novel targets contributing to this disease. One such target, which has been implicated in the etiology of breast cancer, is the fibroblast growth factor (FGF) receptor. FGF receptors (FGFR) as well as a number of FGF ligands, play a critical role in regulating normal mammary gland development and tissue homeostasis (2). There is also increasing evidence for the importance of FGF signaling in human cancers, including breast cancer. High-throughput sequencing studies have shown activating FGF mutations to be highly common in multiple forms of human cancer, including breast cancer (3). Additionally, analysis of copy number abnormalities has shown a consistently high level of amplification of chromosomal region 8p11 containing the *FGFR1* coding region in early-stage breast cancers, resulting in overexpression of FGFR1 (4,5). A multitude of correlative studies has implicated both mammary-specific FGFR subtypes (FGFR1 and FGFR2) in specific subsets of human breast cancer, including luminal A, ER-positive lobular, and low-grade ductal carcinomas (5,6). Single-nucleotide polymorphism (SNP) analysis has identified a relationship between common SNPs in intron 2 of the *FGFR2* gene and increased breast cancer risk possibly as the result of elevated FGFR2 expression (7). Despite increasing evidence implicating altered FGFR expression in human breast cancer, the downstream molecular effects of enhanced FGFR expression remain unclear.

In addition to these clinical studies, the use of genetically engineered mouse (GEM) models has indicated that the FGF pathway, especially in cooperation with the Wnt/β-catenin pathway, plays an important role in mammary tumorigenesis. The Wnt pathway may be commonly activated in breast cancer, possibly as a consequence of the epigenetic silencing of Wnt pathway antagonists, such as SFRP family genes as well as DKK1 (8). Methylation and subsequent inactivation of SFRP1, SFRP2, and SFRP3 have been shown to occur as frequently as 40%, 77%, and 71%, respectively, in primary human breast tumors (8). Additionally, evidence that β-catenin is stabilized in >50% of human breast carcinomas suggests a significant role for the canonical Wnt pathway in this disease (9). Wnt-1, the extracellular ligand and founding member of the Wnt pathway, was originally discovered as a proto-oncogene activated by the random insertion of the mouse mammary tumor virus (MMTV) promoter into the mouse genome, leading to mammary carcinomas (10,11). Early studies on MMTV–Wnt-1 tumors identified FGF3 as a cooperative oncogene selectively activated in ~40% of MMTV-infected, Wnt-1–induced tumors, strongly implicating the two pathways as highly cooperative in breast cancer initiation (12). MMTV insertional mutagenesis studies indicate that activation of Wnt and FGF pathway components is the most common occurrence in resulting tumors (13,14), providing definitive genetic proof for the cooperativity between these two pathways. To eliminate the complexities and redundancies of FGF ligand/receptor interactions, our laboratory has developed and characterized a drug-inducible, ligand-independent FGFR1 model (15–17). In previous studies, treatment with chemical dimerizer AP20187 resulted in rapid hyperplastic progression but was not sufficient for tumorigenesis (16–18). Using these GEM models of

FGFR1 signaling crossed with the MMTV–Wnt-1 (Wnt-1) model, we now show the effect of activating these pathways on mammary tumorigenesis and, for the first time, have begun to elucidate some of the critical mechanisms involved. Activation of inducible FGFR1 (iFGFR1) in the Wnt-1 model resulted in a dramatic reduction in tumor latency and different outcomes in tumor aggressiveness and histology when compared with Wnt-1 tumors alone. Additionally, we observed FGFR-induced protein translation of Wnt/β-catenin oncogenes and discovered a protein translational gene signature that correlated well with enhanced FGFR expression in human breast cancer. Elevated protein translation is highly oncogenic in many different human cancers, including breast cancer. These studies show that one mechanism potentially responsible for the cooperativity and extremely rapid tumorigenesis observed in the iFGFR/MMTV–Wnt-1 bigenic mouse model involves the activation of protein translational pathways, resulting in polysomal recruitment and enhanced expression of several highly oncogenic Wnt/β-catenin mRNAs.

Materials and Methods

Polysomal analysis

Frozen tissue (50 mg) was pulverized under liquid nitrogen and resuspended in 500 μL of cold polysomal lysis buffer (19). Resuspended tissue was placed into a 1-mL Wheaton Dounce homogenizer and vigorously lysed with 100 passes. Samples were spun twice at 16,000 × *g* for 5 minutes at 4°C. The supernatant was loaded on top of an 11-mL 15% to 45% sucrose gradient and ultracentrifuged for 2.5 hours at 38,000 rpm in a SW41Ti rotor (Beckman). The gradient was collected on an ISCO Gradient Fractionator equipped with UA-6 UV spectrophotometer.

Animals, treatments, and cell culture

MMTV-iFGFR1 mice were previously generated and characterized (16,18). All mice were FVB background littermates. Mice were injected i.p. with 1 mg/kg AP20187, a chemical dimerizer for the iFGFR model (Ariad Pharmaceuticals), every 3 days. MCF7 cells were serum starved in serum-free media for 24 to 36 hours before treatment with 100 ng/mL human recombinant FGF2 (Invitrogen) with or without 100 nmol/L PD173074 (Calbiochem).

Immunohistochemistry, immunofluorescence, and quantification

All sections were pretreated using a sodium citrate antigen retrieval protocol as previously described (20). Antibodies were used according to the manufacturer's protocols (Supplementary Table S2).

Quantification of phospho-H3 and bromodeoxyuridine (BrdUrd) at the early time points was obtained by counting three random sections of epithelium for each individual time point. Positive nuclear staining was then quantified for each picture as a percentage of the total area of all blue 4′,6-diamidino-2-phenylindole (DAPI) nuclear staining as described previously (21). At least several hundred cells per picture were counted using Image-Pro Plus software.

Quantitative reverse transcription-PCR

cDNA templates were generated using a SuperScript III kit and 1 μg RNA per sample according to the manufacturer's protocol (Invitrogen). Quantitative PCRs were run using SYBR Green reagent (Applied Biosystems) on a StepOnePlus thermocycler (Applied Biosystems), and fold changes were calculated using the comparative C_T ($\Delta\Delta C_T$) method and StepOne software v2.0.1 (Applied Biosystems). Primer sequences for cMyc, cyclin D1,

and survivin were obtained from (Roche Applied Science), and 18S RNA from Visvader and colleagues. (22).

Immunoblot analysis and quantification

Pulverized, frozen tissue or cells were resuspended in radioimmunoprecipitation assay buffer plus phosphatase (Sigma) and protease (Roche) inhibitors. Cell lysate protein was quantified using the bicinchoninic acid method (Pierce), separated using SDS-PAGE, and transferred to nitrocellulose membranes. All antibodies were used according to the manufacturer's protocols (Supplementary Table S2). Densitometry of exposed films was quantified using Scion Image software (NIH).

Gene microarray expression analysis, data set correlative studies, and statistics

Total RNA (2.5 μg) was reverse transcribed, amplified, and labeled with Cy5 using a Low RNA Input Amplification kit (Agilent), hybridized overnight to Agilent Mouse Oligo Microarrays, and analyzed as described previously (23). The data have been deposited to the Gene Expression Omnibus under the series GSE17916. In the final data set, only genes that reported values in 70% or more of the samples were included. The genes were median centered, and then hierarchical clustering was performed using Cluster v2.12.

To score each of the human breast tumors in a given expression profile data set for similarity to our protein translational gene signature, we derived a “t-score” for the human tumor in relation to the signature, in the same manner to that in previous studies (24,25).

Kaplan-Meier plots and statistical analysis

Kaplan-Meier plots were generated as previously described (26). Significance of fold changes for reverse transcription-PCR (RT-PCR) results was determined using Student's *t* tests. All tests and graphical representation of data were performed using GraphPad Prism.

Results

A marked decrease in tumor latency and increased tumor multiplicity in the MMTV–Wnt-1 × MMTV-iFGFR1 bigenic mice, with differences in tumor aggressiveness and histology

Currently, little is known about the mechanisms leading to FGF/Wnt-induced tumorigenesis. To investigate this, MMTV-iFGFR1/MMTV–Wnt-1 (Wnt/iR1), bigenic, and MMTV–Wnt-1 (Wnt-1) mice were generated and injected every 3 days with dimerizer at 21 days of age. Bigenic Wnt/iR1 mice developed tumors significantly faster than Wnt-1 alone (Fig. 1A). Wnt-1 mice had a mean latency in accordance with previous results (27). Additionally, the average tumor multiplicity was significantly greater in the Wnt/iR1 bigenic mice compared with Wnt-1 alone (3 versus 1, respectively; Fig. 1B), and Wnt/iR1 tumors grew significantly faster than the Wnt-1 tumors (Fig. 1B). In accordance with tumor growth rate, cell proliferation as measured by BrdUrd incorporation was significantly greater in the Wnt/iR1 tumors compared with Wnt-1 alone (Supplementary Fig. S1).

Recent correlative genome-wide studies have implicated FGFR as a potential oncogene in specific subsets of human breast cancer, including luminal A, ER-positive lobular, and low-grade ductal breast carcinomas (4,5). To identify any histologic differences, the tumors were characterized by an expert pathologist (Fig. 1C). Wnt-1 tumors were similar to the classic type P (plaque) tumor associated with MMTV LTR insertional activation of proto-oncogenes such as int-2 (FGF3; ref. 28). The Wnt/iR1 tumors were histologically distinct from Wnt-1 and were classified as a solid tumor, closely resembling the classic ErbB2 type (Fig. 1C; ref. 28). However, both the Wnt-1 and Wnt/iR1 tumors did not express significant levels of ErbB2 (data not shown). The tumors were composed of multiple clusters of solid,

expanding nodules of cells with zonal organization. They contained frequent pockets of necrosis, possibly the result of reduced angiogenesis observed throughout the tumor mass (Supplementary Fig. S2).

Analysis of copy number abnormalities in various human breast pathologies has identified the amplification of chromosomal region 8p12-11 containing the coding region of *FGFR1* to be associated with adverse patient outcome and distant recurrence of the luminal A subtype (4,6). Accordingly, tumors were double stained for luminal marker K18 and myoepithelial (basal) marker K5 to determine the luminal/basal status of the two tumor types (Fig. 1D). We observed an expansion of the $K18^+$ cells in the Wnt/iR1 bigenic tumors compared with Wnt-1 alone. This was characterized by the disruption of the $K5^+$ layer in the Wnt/iR1 tumors, which remained mostly intact in the Wnt-1 tumors. To confirm the association of the hemagglutinin (HA)–tagged iFGFR with luminal-like cell expansion, we performed double immunofluorescence costaining for either luminal marker K8 and HA tag or basal marker K5 and HA tag (Supplementary Fig. S3). We observed a very strong correlation between K8 staining and expression of the HA tag and no correlation between K5 staining and expression of the HA tag, indicating the expression of the iFGFR only in the luminal-like epithelium.

iFGFR1 activation leads to rapid mammary epithelial expansion in bigenic mice

Due to the extremely rapid palpable tumor formation observed in the bigenic Wnt/iR1 mice, we wanted to observe the early effects of dimerizer-induced iFGFR1 activation. Twenty-eight-day-old wild-type, Wnt-1, and Wnt/iR1 mice were injected with dimerizer, and their number 4 inguinal mammary glands were removed before or 6, 24, and 48 hours following treatment. Before dimerizer treatment, mammary gland whole mounts and H&E sections from Wnt-1 and Wnt/iR1 mice displayed hyperplasia throughout the gland as previously observed in the Wnt-1 model (Fig. 2; refs. 10,29). Wnt/iR1 glands were more hyperplastic than the Wnt-1 glands and showed some areas of “thickening” of the epithelial ducts close to the nipple, most likely due to some leaky, drug-independent dimerization of iFGFR1, although this was observed albeit less frequently in the Wnt-1 mice (Fig. 2A, white arrows). Surprisingly, within 24 hours of dimerizer treatment, a dramatic expansion of the mammary epithelium was observed in the majority of bigenic Wnt/iR1 glands, leading to the formation of large solid nodules by 48 hours, well before the developing epithelium was able to extend to the lymph node. Expansion of the Wnt/iR1 epithelium seemed to occur throughout the entire gland, leading to the formation of multiple clusters of nodules (Fig. 2A, red arrow), eventually crowding together to form the distinctive nodular-like histology previously described. Histologic analysis showed this expansion to lead to the complete loss of the luminal compartment, which became filled with the expanding cells (Fig. 2B, asterisk). The rapid expansion was also confirmed in individual mice by ultrasound imaging (Supplementary Fig. S4). Immunofluorescence staining and quantification of the mitotic marker phospho-H3 and S-phase marker BrdUrd showed a dramatic peak in cell proliferation 24 hours following dimerizer treatment within the expanded Wnt/iR1 epithelium but not the Wnt-1 epithelium (Fig. 2C and D). This marked increase in proliferation directly correlated with the epithelial expansion seen at 24 hours in the bigenic Wnt/iR1 mice, suggesting that the expansion was caused by rapid entry of quiescent cells into the cell cycle.

Microarray analysis reveals a distinct protein translational gene signature within Wnt/iR1 tumors

To investigate any changes in gene expression, significance analysis of microarrays was performed to compare Wnt-1 tumors only versus Wnt/iFGFR1/FGFR2-induced tumors. This analysis yielded 1,485 genes that were upregulated and 910 downregulated in Wnt/iFGFR

tumors compared with Wnt-1 alone with a false discovery rate of 1.74%. This gene list was then analyzed using Ingenuity Pathway Analysis software. Interestingly, genes known to be direct targets of Wnt/β-catenin signaling implicated in various human cancers and development were largely unaffected by iFGFR signaling in our model (30). Additionally, there was no observable change in membrane or nuclear localization of β-catenin or any increase in dephosphorylated active β-catenin in the Wnt/iFGFR tumors versus the Wnt-1 tumors (data not shown). These results suggest that the mechanisms of iFGFR and Wnt/β-catenin cooperativity might involve posttranscriptional regulation. Interestingly, among the top Molecular and Cellular Functions and Networks ranked by Ingenuity was a distinct protein synthesis signature (Supplementary Fig. S5).

Cluster analysis comparing 20 genes identified by Ingenuity Pathway Analysis as important in protein translation showed a significant shift in expression on activation of iFGFR (Fig. 3; Supplementary Table S1). These included components of the translational machinery, such as eukaryotic initiation factors (eIF), and critical regulators of translational initiation, such as *eIF4E-binding proteins* (*eIF4E-BP*) as well as *S6-ribosomal protein* (*S6-RP*; ref. 31). Importantly, previously published microarray analysis of dimerizer-treated MMTV-iFGFR1 mice did not show any significant induction of these translational regulators at the RNA level (data not shown; ref. 18). However, this may be a result of the low ratio of epithelium to fat pad in nontransformed glands in virgin mice. In support of this hypothesis, increased expression of several translational regulators identified in our gene signature was observed within 2 hours following dimerizer treatment of HC11 mammary epithelial cells stably expressing iFGFR1 (data not shown). These included EIF1α, EIF4-BP1, eIF4E, and EIF5b. These results suggest that iFGFR1 signaling can directly induce expression of these translational regulators.

iFGFR1 signaling leads to increased polysomal loading and protein expression of several Wnt/β-catenin target mRNAs

The change in regulation of a number of critical translational machinery components led us to suspect that a critical element of iFGFR1 signaling, contributing to and maintaining enhanced cellular proliferation, might be translational regulation rather than transcriptional cooperativity. To investigate this, we analyzed three Wnt/β-catenin target oncogenes known to be both highly translationally regulated and critical in driving cell cycle progression: cMyc, survivin, and cyclin D1 (32,33). We first established through quantitative PCR that these genes were not being upregulated at the mRNA level, and in fact, in accordance with our microarray data, cyclin D1 mRNA levels were actually decreased in the Wnt/iR1 tumors (Fig. 4A). We then performed immunoblots on cell lysates using three pools of three independent tumors from both the Wnt-1 and Wnt/iR1 groups (Fig. 4B). Within all three pools, the Wnt/iR1 tumors displayed elevated cMyc levels. Two of the three Wnt/iR1 pools that had elevated survivin and cyclin D1 levels were similar between all groups. Densitometry analysis of multiple tumors showed about a 2-fold enrichment of cMyc and survivin and similar expression of cyclin D1 when normalized to cyclophilin (Fig. 4B). These results suggested that there was a selective increase in protein expression relative to mRNA, an indication of posttranscriptional upregulation in the Wnt/iR1 tumors.

One of the best indications of translational upregulation of specific mRNA species is their selective recruitment to multiple ribosomes or polyribosomes (polysomes; refs. 19,34,35). Due to differences in density, mRNA species bound by one or multiple ribosomes can be sedimented on differential sucrose gradients through ultracentrifugation and interrogated through quantitative PCR, microarray analysis, or sequencing (19,34,36). We adapted this method to investigate the difference in expression levels of select mRNAs specifically bound to polysomes within the Wnt-1 and Wnt/iR1 tumors (Fig. 4C; see Materials and Methods for details). Absorbance (260 nm) readings were measured throughout collection,

generating a distinctive polysomal profile with 40S, 80S, and polysomal peaks (Fig. 4C, first arrow, second arrow, and asterisk, respectively). mRNA was extracted from each sucrose fraction, and quantitative PCR analysis comparing RNA fold changes of cMyc, survivin, and cyclin D1 between each fraction indicated a dramatic shift from reduced mRNA in fractions 1 to 4 to increased mRNA in fractions 5 to 9 in the Wnt/iR1 tumors over the Wnt-1 tumors (Fig. 4D; Supplementary Fig. S6). These results show a decrease in soluble, nonpolysome-bound mRNA of our target oncogenes (fractions 1–4) and an increase in polysome-bound mRNA (fractions 5–9) within the Wnt/iR1 tumors, indicating the preferential recruitment of these mRNA species to polysomes. cMyc, survivin, and cyclin D1 showed cumulative fold changes from unbound to bound of +9.6 ± 2.5 for cMyc, +4.2 ± 1.5 for survivin, and +4.1 ± 1.3 for cyclin D1 within the Wnt/iR1 tumors versus Wnt-1. Cyclophilin, whose protein expression did not change between tumor types, did not show this shift (Supplementary Fig. S6). Importantly, the increased protein levels of cMyc and survivin correlated directly with the increased fold change of mRNA in the polysome fractions. Cyclin D1 mRNA did not increase in the Wnt/iR1 polysome fractions, correlating with the similar protein levels between the two tumor types. However, because whole-cell cyclin D1 mRNA levels were reduced, but protein levels were similar, cyclin D1 mRNA apparently was recruited more efficiently to polysomes in the Wnt/iR1 tumors. In addition, peak polysome loading of cMyc mRNA was observed in fractions 8 and 9 compared with a peak in survivin mRNA at around fractions 5 and 6. This was expected because the cMyc transcript is almost three times larger than the survivin mRNA, allowing increased ribosome loading.

iFGFR1 activation leads to increased phosphorylation of critical translational regulators and a rapid increase in cMyc and survivin protein levels in bigenic mice

Phosphorylation of critical translational machinery is a common regulatory mechanism observed following activation of the oncogenic AKT and extracellular signal-regulated kinase (ERK) pathways. This can result in both a global increase in protein translation and selective translation of specific progrowth mRNAs (31). We used immunohistochemistry with phospho-specific antibodies to analyze Wnt-1 and Wnt/iR1 tumors and found an increase in active phosphorylated forms of several different translational regulators in the Wnt/iR1 tumors, despite relatively similar levels of endogenous nonphosphorylated protein (Fig. 5A; Supplementary Fig. S7). Additionally, immunoblot analysis on mammary gland lysates from dimerizer-treated 28-day-old Wnt-1 and Wnt/iR1 mice showed a peak in phospho-ERK at 6 hours and phospho-ERK targets MNK and eIF4E within 24 hours following treatment. Phospho-AKT levels increased from 6 to 24 hours along with translational regulator S6-RP in the Wnt/iR1 mice (Fig. 5B). Phosphorylation of these factors was not increased as a result of dimerizer treatment in the Wnt-1 mice. Concurrent with the increase in phosphorylated ERK, AKT, and translation factors, cMyc and survivin protein levels were increased 6 hours following dimerizer treatment and continued to increase up to 24 hours. As expected, cyclin D1 protein levels remained constant. The observed increase by 6 hours in cMyc and survivin protein levels, along with the concurrent activation of phospho-ERK, phospho-AKT, phospho– S6-RP, and eIF4E, suggests that these events may play a critical role in regulating the rapid increase in epithelial cell proliferation. Activation of these translational regulators was observed *in vitro* using endogenous FGFR/FGF signaling in the human MCF7 breast cancer cell line on treatment with FGF2 following a period of serum starvation (Supplementary Fig. S8). Due to the limitation of mice as well as the inability to get a precise picture of the kinetics of phosphorylation involved *in vivo*, this *in vitro* model provided a useful surrogate to study the kinetics of phosphorylation of the different translational regulatory components downstream from ERK and/or AKT signaling.

Elevated FGFR1 and FGFR2 expression levels correlate with a protein translation gene signature in human breast cancer

Microarray analysis of Wnt/iFGFR bigenic tumors versus Wnt-1 alone revealed a distinctive protein translational gene signature (Fig. 3). We compared this signature to FGFR1 or FGFR2 expression in several different microarray data sets consisting of hundreds of human breast cancer samples (Fig. 6; Table 1; refs. 37–41). Each tumor in five independent breast tumor data sets was scored for similarity with the protein translational gene signature; this score provides a measure of how the tumor recapitulated the patterns of overexpression and underexpression observed in the translation signature. The majority of the data sets displayed a significant correlation between elevated FGFR1 or FGFR2 expression and the translational gene signature, suggesting that these genes may play a role in the manifestation of human breast cancers with elevated FGFR1 and/or FGFR2 (Fig. 6; Table 1). We decided to analyze two other tyrosine kinase receptors: epidermal growth factor receptor (EGFR) and ErbB2. Whereas EGFR was also shown to significantly correlate with the protein translational signature, surprisingly ErbB2 showed a negative correlation (Supplementary Table S3). These results indicate that there are distinct differences between these receptor tyrosine kinase signaling pathways with respect to their translational regulatory activity in human breast cancer.

Discussion

Although increasing evidence implicates FGFR in the etiology of human breast cancer, the mechanisms underlying its involvement have yet to be elucidated. Mouse models, like the ones used in these studies, provide valuable tools to decipher the function of conserved pathways such as FGF and Wnt in human cancer. The fact that random insertion of the MMTV provirus in the mouse genome consistently generates tumors with simultaneous activation of both Wnt and FGF ligands suggests that these two pathways are highly collaborative in the initiation of mammary tumorigenesis (10,13). Although previous studies provide evidence for the existence of FGF and Wnt pathway cooperation, they fail to elucidate potential mechanisms responsible for this cooperativity. Previous studies in nulliparous animals showed that chronic iFGFR1 activation resulted in hyperplasia but was not sufficient to cause palpable tumor formation (16,18,42). Thus, the rapidity at which palpable tumors developed in the Wnt/iR1 bigenic mice on dimerizer treatment was quite unexpected. Based on these results, we decided to examine the changes, which occurred immediately following dimerizer treatment, and uncovered an unprecedented expansion of the mammary epithelium resulting from activation of these two pathways. This, therefore, provided an excellent model in which to investigate the potential mechanisms involved.

Several studies investigating tumor initiation in the MMTV–Wnt-1 mouse model have implicated secondary activating mutations in *Hras1* and *Kras2* in ~50% of MMTV–Wnt-1–induced tumors (43,44). These mutations were shown to result in greater sustained activation of phospho-ERK and phospho–phosphatidylinositol 3-kinase (PI3K)/AKT pathways (44). In the current studies, the tumors did not originate from a clonal cell population. The rapid and widespread activation of cell proliferation observed throughout the gland suggests that secondary mutations are not required in this case for tumorigenesis, highlighting the importance of cooperativity between these two pathways. Importantly, the FGF signaling pathway, known to activate both ERK and PI3K/AKT, seems to have obviated the requirement for secondary mutations needed to activate these pathways. In fact, a very strong correlation was observed between ERK pathway activation and cell proliferation in the Wnt/iR1 tumors (data not shown).

We initially hypothesized that increased β-catenin stabilization and resultant canonical Wnt target gene transcription might be the primary mechanism contributing to the FGF/Wnt

cooperativity. Previous studies have shown that the inhibition of glycogen synthase kinase 3 as a consequence of insulin-like growth factor-I/protein kinase B/AKT or ERK-mediated phosphorylation of $Ser^{21/9}$ residues resulted in enhanced β-catenin stabilization (45). However, microarray analysis did not reveal any significant change in Wnt/β-catenin target gene expression as a result of iFGFR signaling in bigenic mice, nor did we observe any differences in β-catenin stabilization. Interestingly, this suggested that much of the cooperativity between these two pathways may have been through posttranscriptional mechanisms. The highly significant protein translational gene signature identified through pathway analysis of the microarray results also suggested that iFGFR1 activation of protein synthesis might enhance mammary tumorigenesis in the bigenic mice. However, it is not clear if this gene signature is the result of direct FGFR signaling inducing gene expression or an indirect effect as a result of a positive feedback mechanism. In support of the first hypothesis, a 2-hour treatment with dimerizer in iFGFR1-expressing HC11 cells resulted in the transcriptional activation of several translational regulators identified in our signature, such as EIF1α, eIF4E-BP, eIF4E, and EIF5b (data not shown). Alternatively, increased levels of cMyc have been reported to exert a general effect on translational efficiency (46). Thus, it is possible that this translational signature reflects both direct and indirect effects of FGFR1 signaling.

Oncogenic ras, AKT, and ERK signaling have all been shown to contribute to the selective translation of oncogenic mRNAs such as cMyc and cyclin D1 in human glioblastoma tissue and cell lines (32,34). Downstream phosphorylation of critical translational regulatory components such as mammalian target of rapamycin (mTOR), eIFs, ribosomal proteins such as S6-RP, and their inhibitors are key regulators involved in the specific recruitment of progrowth mRNA species to polysomes. In fact, many of these factors and their phosphorylated forms are upregulated in various human cancers, including breast cancer (33,47,48). Phosphorylation of these components through AKT-mTOR or ERK-MNK signaling has been shown to enhance the specific translation of oncogenic “inefficiently translated” mRNAs with G/C-rich 5′ untranslated regions and reduces the translation of more “efficiently translated” mRNA species not involved in cell cycle progression or survival (33,47,48). Interestingly, in recent studies using iFGFR1-transformed MCF10A cells and a cell line derived from a human lobular carcinoma, known to have a copy number amplification of FGFR1, a dependence on ribosomal S6 kinase (RSK) activity for FGFR1-incurred growth and survival was observed (49). In agreement with these results, we now show that iFGFR1 enhances phosphorylation of S6-RP, a direct RSK phospho-target. Whether the RSK dependence observed in breast cancers with activated FGFR1 requires the selective translational recruitment of progrowth and prosurvival genes remains to be established.

In summary, the current studies show that FGFR signaling leads to increased phosphorylation and transcription of key translational regulators and recruitment of several Wnt/β-catenin target mRNAs to polysomes on sustained signaling, along with the rapid appearance of palpable tumors. The expression of oncogenes, such as cMyc, survivin, and cyclin D1, is regulated by multiple mechanisms and signaling pathways in addition to the translational mechanisms described in this study. Furthermore, FGF signaling is known to regulate many factors important for mammary tumorigenesis, including macrophage recruitment and angiogenesis (17,35). However, because of the rapid effects observed on tumorigenesis in these bigenic mice, FGFR-induced protein synthesis, including translational upregulation of Wnt/β-catenin target oncogenes, already induced at the transcriptional level may play a critical role in driving and sustaining the rapid tumor growth observed. These translational effects are most likely not limited to Wnt/β-catenin target genes alone. Future bioinformatic studies of large-scale changes to the proteome and next-generation sequencing of polysomal mRNAs performed at different times following FGFR

activation using the bigenic mouse model will be required to provide a more complete picture of translationally regulated mRNAs.

It is not surprising that rapid and sustained induction of cell proliferation may be dependent on new protein synthesis. In fact, the effects of AKT signaling on polysomal recruitment of specific mRNAs have been shown previously to occur as rapidly as 2 hours following activation before major changes in gene transcription (34). In addition, cells proliferating at a very high rate are dependent on the continued production of new proteins necessary for both basic cellular functions as well as cell cycle regulators and oncogenes, which would otherwise be lost after successive cell divisions. It is likely that the general inhibition of protein translation will attenuate tumor growth in our mouse model as observed for other studies of tumor growth both *in vitro* and *in vivo*. Interestingly, early clinical trials with the first generation of protein synthesis inhibitors targeting eIF4E in several cancers, including breast cancer, are currently being initiated (50).

Traditionally, most studies investigating changes in gene regulation involved in tumorigenesis have focused almost exclusively on gene expression profiling, with much less attention on changes in protein synthesis and activity. Interestingly, novel high-throughput studies using nextgeneration sequencing and ribosomal recruitment assays recently have shown that it is possible to interrogate global changes in the yeast proteome on starvation conditions (36). In the future, these types of studies should provide new insights into the role translational regulation plays in the etiology of breast cancer, potentially providing additional targets for adjuvant therapy. The current studies further extend our understanding of FGFR signaling in the etiology of breast cancer and provide an excellent model to undertake future studies of global changes in the breast cancer proteome as a function of oncogenic FGF signaling. Fortunately, FGFRs, like other receptor tyrosine kinases, notably ErbB2, may provide druggable targets for adjuvant therapy, and there are several known FGFR inhibitors currently in clinical trials. Additionally, small-molecule inhibitors regulating the key pathways involved in translation initiation also may provide new therapeutic targets for human breast cancers with alterations in FGFR signaling.

Supplementary Material

Refer to Web version on PubMed Central for supplementary material.

Acknowledgments

We thank all members of the Rosen lab, especially Shirley Small, Maria Gonzalez-Rimbau, and Stephanie Green, for their technical support; Baylor Mouse Phenotyping Core for their help with our ultrasound imaging; and Drs. David Spencer, David Rowley, Yi Li, and Thomas Zwaka for their insights and comments. We would also like to thank ARIAD Pharmaceuticals for supplying chemical dimerizer AP20187.

Grant Support

NIH grant R37 CA16303 from the National Cancer Institute (J.M. Rosen).

References

1. Schlotter CM, Vogt U, Allgayer H, Brandt B. Molecular targeted therapies for breast cancer treatment. Breast Cancer Res. 2008; 10:211. [PubMed: 18671839]
2. Grose R, Dickson C. Fibroblast growth factor signaling in tumorigenesis. Cytokine Growth Factor Rev. 2005; 16:179–186. [PubMed: 15863033]
3. Greenman C, Stephens P, Smith R, et al. Patterns of somatic mutation in human cancer genomes. Nature. 2007; 446:153–158. [PubMed: 17344846]

4. Chin K, DeVries S, Fridlyand J, et al. Genomic and transcriptional aberrations linked to breast cancer pathophysiologies. Cancer Cell. 2006; 10:529–541. [PubMed: 17157792]
5. Reis-Filho JS, Simpson PT, Turner NC, et al. FGFR1 emerges as a potential therapeutic target for lobular breast carcinomas. Clin Cancer Res. 2006; 12:6652–6662. [PubMed: 17121884]
6. Adelaide J, Finetti P, Bekhouche I, et al. Integrated profiling of basal and luminal breast cancers. Cancer Res. 2007; 67:11565–11575. [PubMed: 18089785]
7. Meyer KB, Maia AT, O'Reilly M, et al. Allele-specific up-regulation of FGFR2 increases susceptibility to breast cancer. PLoS Biol. 2008; 6:e108. [PubMed: 18462018]
8. Suzuki H, Toyota M, Carraway H, et al. Frequent epigenetic inactivation of Wnt antagonist genes in breast cancer. Br J Cancer. 2008; 98:1147–1156. [PubMed: 18283316]
9. Lin SY, Xia W, Wang JC, et al. β-Catenin, a novel prognostic marker for breast cancer: its roles in cyclin D1 expression and cancer progression. Proc Natl Acad Sci U S A. 2000; 97:4262–4266. [PubMed: 10759547]
10. Nusse R, Varmus HE. Many tumors induced by the mouse mammary tumor virus contain a provirus integrated in the same region of the host genome. Cell. 1982; 31:99–109. [PubMed: 6297757]
11. Brennan KR, Brown AM. Wnt proteins in mammary development and cancer. J Mammary Gland Biol Neoplasia. 2004; 9:119–131. [PubMed: 15300008]
12. Shackleford GM, MacArthur CA, Kwan HC, Varmus HE. Mouse mammary tumor virus infection accelerates mammary carcinogenesis in Wnt-1 transgenic mice by insertional activation of int-2/Fgf-3 and hst/Fgf-4. Proc Natl Acad Sci U S A. 1993; 90:740–744. [PubMed: 8380647]
13. Theodorou V, Kimm MA, Boer M, et al. MMTV insertional mutagenesis identifies genes, gene families and pathways involved in mammary cancer. Nat Genet. 2007; 39:759–769. [PubMed: 17468756]
14. Lee FS, Lane TF, Kuo A, Shackleford GM, Leder P. Insertional mutagenesis identifies a member of the Wnt gene family as a candidate oncogene in the mammary epithelium of int-2/Fgf-3 transgenic mice. Proc Natl Acad Sci U S A. 1995; 92:2268–2272. [PubMed: 7892260]
15. Xian W, Schwertfeger KL, Rosen JM. Distinct roles of fibroblast growth factor receptor 1 and 2 in regulating cell survival and epithelial-mesenchymal transition. Mol Endocrinol. 2007; 21:987–1000. [PubMed: 17284663]
16. Welm BE, Freeman KW, Chen M, Contreras A, Spencer DM, Rosen JM. Inducible dimerization of FGFR1: development of a mouse model to analyze progressive transformation of the mammary gland. J Cell Biol. 2002; 157:703–714. [PubMed: 12011115]
17. Xian W, Schwertfeger KL, Vargo-Gogola T, Rosen JM. Pleiotropic effects of FGFR1 on cell proliferation, survival, and migration in a 3D mammary epithelial cell model. J Cell Biol. 2005; 171:663–673. [PubMed: 16301332]
18. Schwertfeger KL, Xian W, Kaplan AM, Burnett SH, Cohen DA, Rosen JM. A critical role for the inflammatory response in a mouse model of preneoplastic progression. Cancer Res. 2006; 66:5676–5685. [PubMed: 16740705]
19. del Prete MJ, Vernal R, Dolznig H, Mullner EW, Garcia-Sanz JA. Isolation of polysome-bound mRNA from solid tissues amenable for RT-PCR and profiling experiments. RNA. 2007; 13:414–421. [PubMed: 17237355]
20. Grimm SL, Contreras A, Barcellos-Hoff MH, Rosen JM. Cell cycle defects contribute to a block in hormone-induced mammary gland proliferation in CCAAT/enhancer-binding protein (C/EBPβ)-null mice. J Biol Chem. 2005; 280:36301–36309. [PubMed: 16120603]
21. Heckman BM, Chakravarty G, Vargo-Gogola T, et al. Crosstalk between the p190-B RhoGAP and IGF signaling pathways is required for embryonic mammary bud development. Dev Biol. 2007; 309:137–149. [PubMed: 17662267]
22. Visvader JE, Venter D, Hahm K, et al. The LIM domain gene LMO4 inhibits differentiation of mammary epithelial cells *in vitro* and is overexpressed in breast cancer. Proc Natl Acad Sci U S A. 2001; 98:14452–14457. [PubMed: 11734645]
23. Herschkowitz JI, Simin K, Weigman VJ, et al. Identification of conserved gene expression features between murine mammary carcinoma models and human breast tumors. Genome Biol. 2007; 8:R76. [PubMed: 17493263]

24. Creighton CJ, Casa A, Lazard Z, et al. Insulin-like growth factor-I activates gene transcription programs strongly associated with poor breast cancer prognosis. J Clin Oncol. 2008; 26:4078–4085. [PubMed: 18757322]
25. Gibbons DL, Lin W, Creighton CJ, et al. Expression signatures of metastatic capacity in a genetic mouse model of lung adenocarcinoma. PLoS One. 2009; 4:e5401. [PubMed: 19404390]
26. Massarweh S, Osborne CK, Jiang S, et al. Mechanisms of tumor regression and resistance to estrogen deprivation and fulvestrant in a model of estrogen receptor-positive, HER-2/neu-positive breast cancer. Cancer Res. 2006; 66:8266–8273. [PubMed: 16912207]
27. Li Y, Hively WP, Varmus HE. Use of MMTV-Wnt-1 transgenic mice for studying the genetic basis of breast cancer. Oncogene. 2000; 19:1002–1009. [PubMed: 10713683]
28. Cardiff RD, Anver MR, Gusterson BA, et al. The mammary pathology of genetically engineered mice: the consensus report and recommendations from the Annapolis meeting. Oncogene. 2000; 19:968–988. [PubMed: 10713680]
29. Kwan H, Pecenka V, Tsukamoto A, et al. Transgenes expressing the Wnt-1 and int-2 proto-oncogenes cooperate during mammary carcinogenesis in doubly transgenic mice. Mol Cell Biol. 1992; 12:147–154. [PubMed: 1530875]
30. Logan CY, Nusse R. The Wnt signaling pathway in development and disease. Annu Rev Cell Dev Biol. 2004; 20:781–810. [PubMed: 15473860]
31. Sonenberg N, Hinnebusch AG. Regulation of translation initiation in eukaryotes: mechanisms and biological targets. Cell. 2009; 136:731–745. [PubMed: 19239892]
32. Shi Y, Sharma A, Wu H, Lichtenstein A, Gera J. Cyclin D1 and c-myc internal ribosome entry site (IRES)-dependent translation is regulated by AKT activity and enhanced by rapamycin through a p38 MAPK- and ERK-dependent pathway. J Biol Chem. 2005; 280:10964–10973. [PubMed: 15634685]
33. Graff JR, Konicek BW, Carter JH, Marcusson EG. Targeting the eukaryotic translation initiation factor 4E for cancer therapy. Cancer Res. 2008; 68:631–634. [PubMed: 18245460]
34. Rajasekhar VK, Viale A, Socci ND, Wiedmann M, Hu X, Holland EC. Oncogenic Ras and Akt signaling contribute to glioblastoma formation by differential recruitment of existing mRNAs to polysomes. Mol Cell. 2003; 12:889–901. [PubMed: 14580340]
35. Lin CJ, Cencic R, Mills JR, Robert F, Pelletier J. c-Myc and eIF4F are components of a feedforward loop that links transcription and translation. Cancer Res. 2008; 68:5326–5334. [PubMed: 18593934]
36. Ingolia NT, Ghaemmaghami S, Newman JR, Weissman JS. Genomewide analysis *in vivo* of translation with nucleotide resolution using ribosome profiling. Science. 2009; 324:218–223. [PubMed: 19213877]
37. Wang Y, Klijn JG, Zhang Y, et al. Gene-expression profiles to predict distant metastasis of lymph-node-negative primary breast cancer. Lancet. 2005; 365:671–679. [PubMed: 15721472]
38. van de Vijver MJ, He YD, van't Veer LJ, et al. A gene-expression signature as a predictor of survival in breast cancer. N Engl J Med. 2002; 347:1999–2009. [PubMed: 12490681]
39. Loi S, Haibe-Kains B, Desmedt C, et al. Definition of clinically distinct molecular subtypes in estrogen receptor-positive breast carcinomas through genomic grade. J Clin Oncol. 2007; 25:1239–1246. [PubMed: 17401012]
40. Hoadley KA, Weigman VJ, Fan C, et al. EGFR associated expression profiles vary with breast tumor subtype. BMC Genomics. 2007; 8:258. [PubMed: 17663798]
41. Desmedt C, Piette F, Loi S, et al. Strong time dependence of the 76- gene prognostic signature for node-negative breast cancer patients in the TRANSBIG multicenter independent validation series. Clin Cancer Res. 2007; 13:3207–3214. [PubMed: 17545524]
42. Acevedo VD, Gangula RD, Freeman KW, et al. Inducible FGFR-1 activation leads to irreversible prostate adenocarcinoma and an epithelial-to-mesenchymal transition. Cancer Cell. 2007; 12:559–571. [PubMed: 18068632]
43. Podsypanina K, Li Y, Varmus HE. Evolution of somatic mutations in mammary tumors in transgenic mice is influenced by the inherited genotype. BMC Med. 2004; 2:24. [PubMed: 15198801]

44. Jang JW, Boxer RB, Chodosh LA. Isoform-specific ras activation and oncogene dependence during MYC- and Wnt-induced mammary tumorigenesis. Mol Cell Biol. 2006; 26:8109–8121. [PubMed: 16908535]
45. Desbois-Mouthon C, Cadoret A, Blivet-Van Eggelpoel MJ, et al. Insulin and IGF-1 stimulate the β-catenin pathway through two signalling cascades involving GSK-3β inhibition and Ras activation. Oncogene. 2001; 20:252–259. [PubMed: 11313952]
46. Stoelzle T, Schwarb P, Trumpp A, Hynes NE. c-Myc affects mRNA translation, cell proliferation and progenitor cell function in the mammary gland. BMC Biol. 2009; 7:63. [PubMed: 19785743]
47. Armengol G, Rojo F, Castellvi J, et al. 4E-binding protein 1: a key molecular “funnel factor” in human cancer with clinical implications. Cancer Res. 2007; 67:7551–7555. [PubMed: 17699757]
48. Pyronnet S, Imataka H, Gingras AC, Fukunaga R, Hunter T, Sonenberg N. Human eukaryotic translation initiation factor 4G (eIF4G) recruits mnk1 to phosphorylate eIF4E. EMBO J. 1999; 18:270–279. [PubMed: 9878069]
49. Xian W, Pappas L, Pandya D, et al. Fibroblast growth factor receptor 1-transformed mammary epithelial cells are dependent on RSK activity for growth and survival. Cancer Res. 2009; 69:2244–2251. [PubMed: 19258500]
50. Culjkovic B, Borden KL. Understanding and targeting the eukaryotic translation initiation factor eIF4E in head and neck cancer. J Oncol. 2009; 2009:981679. [PubMed: 20049173]

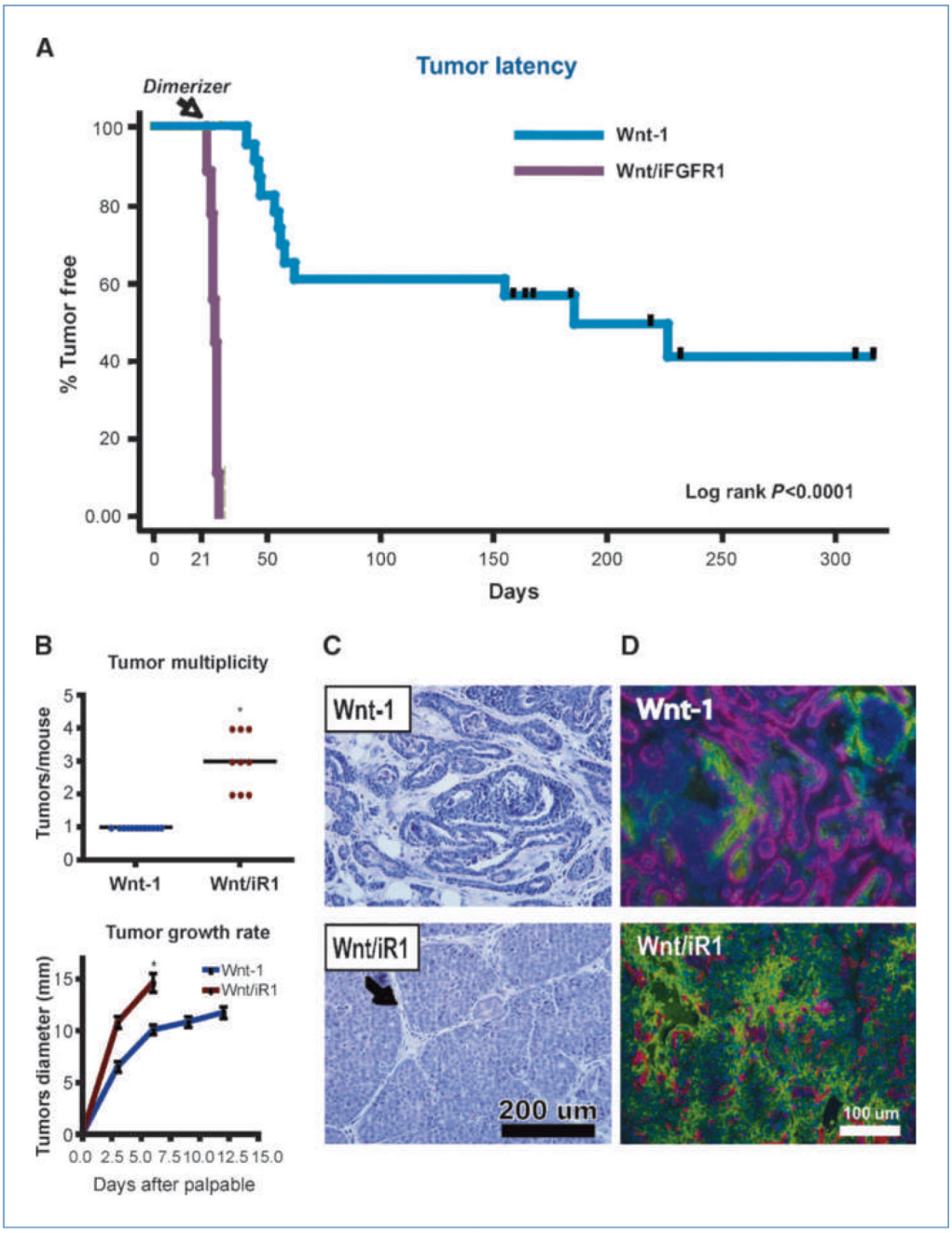

Figure 1.

Activation of iFGFR1 signaling synergizes with Wnt-1 signaling, leading to reduced tumor latency with differences in tumor growth rate, multiplicity, and histologic features. A, Kaplan-Meier plot of tumor incidence of Wnt/iR1 (n = 9 of 9) and Wnt-1 (n = 12 of 23) mice. $P < 0.0001$, log-rank test, Wnt-1 versus Wnt/iR1. B, Wnt/iR1 mice had an average of three tumors per mouse at the time of sacking (n = 9) and Wnt-1 consistently had one tumor per mouse at the time of sacking (n = 12). *, $P < 0.0001$. Wnt/iR1 (n = 9) and Wnt-1 (n = 12) tumor diameter was measured. *, $P < 0.0001$. Points, mean; bars, SE. C, H&E of Wnt/iR1 and Wnt-1 tumor sections. Wnt/iR1 tumors are composed of distinct lobules resulting from the expansion of epithelium (arrow). D, immunofluorescence double staining of

luminal K18 (green) and myoepithelial K5 markers (red) in the different tumor types. Nuclear staining is shown in blue (DAPI).

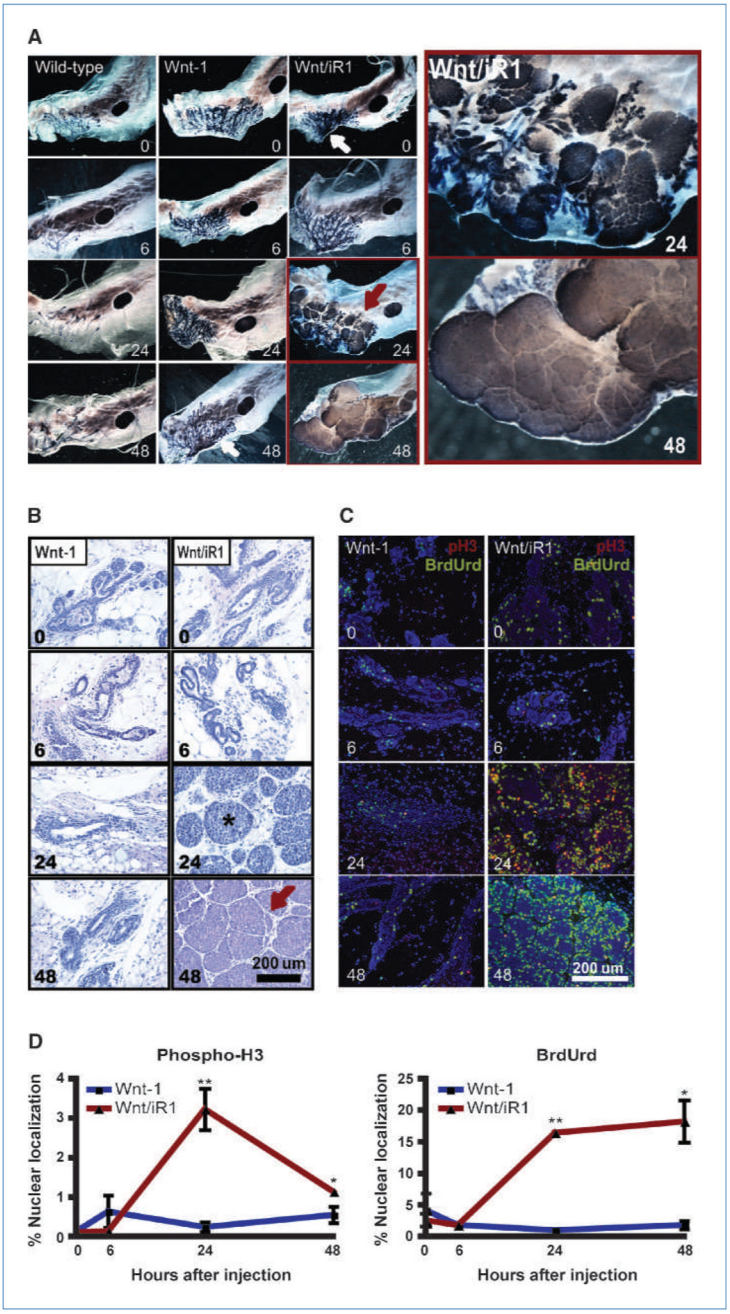

Figure 2.

Activation of iFGFR1 leads to rapid tumor formation and cell proliferation in the Wnt-1 tumor model. A, hematoxylin-stained whole-mount images of number 4 inguinal mammary glands following dimerizer treatment showing rapid epithelial expansion (red arrow). White arrow, ductal thickening. B, H&E staining of number 4 inguinal mammary gland sections following dimerizer treatment showing a rapid epithelial expansion resulting in zonal organization (asterisk). C, immunofluorescence double staining of mitotic marker phospho-H3 (red) and S-phase marker BrdUrd (green) in number 4 inguinal mammary gland sections following dimerizer treatment. Nuclear staining is shown in blue (DAPI). D, quantification of immunofluorescence double staining of nuclear phospho-H3 and BrdUrd in number 4

inguinal mammary gland sections following dimerizer. Phospho-H3 (n = 3 independent sections): **, $P < 0.01$; *, $P < 0.06$, Wnt/iR1 versus Wnt-1. BrdUrd (n = 3 independent sections): **, $P < 0.0001$; *, $P < 0.01$, Wnt/iR1 versus Wnt-1. Points, mean; bars, SE.

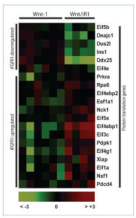

Figure 3.
mRNA expression levels in Wnt/iR1 determined through microarray analysis of tumors identifies changes in genes involved in protein translation. Heat map showing 20 genes differentially expressed in Wnt/iR1 and Wnt-1 tumors. Genes were identified by Ingenuity Pathway Analysis as important in protein translation.

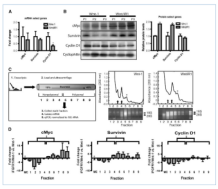

Figure 4.

iFGFR1 signaling leads to increased polysomal loading and protein expression of direct Wnt/β-catenin target oncogenes. A, quantitative RT-PCR analysis of cMyc, survivin, and cyclin D1 (*, $P < 0.05$) normalized to cyclophilin A ($n \geq 4$). Columns, mean; bars, SE. B, immunoblot analysis and quantification of three different direct Wnt/β-catenin target oncogenes from three different pools of three Wnt-1 and three Wnt/iR1 tumors. Cyclophilin A was used as a loading control. Densitometry quantification of cMyc (**, $P < 0.0001$), survivin (*, $P < 0.05$), and cyclin D1 relative protein levels from multiple tumors ($n \geq 3$). Densitometry values from the three genes were normalized to total cyclophilin A protein. Comparisons represent Wnt/iR1 versus Wnt-1 for each gene. Columns, mean; bars, SE. C, schematic illustration of the method used to analyze specific polysome-bound mRNAs in both tumor types. Quantitative RT-PCR results were normalized to 18S rRNA to compensate for global changes in ribosome content per fraction and sample. Figure adapted from del Prete and colleagues (19). Absorbance (260 nm) readings were collected continually across the sucrose gradient to determine the fractions containing the 40S (left arrow), 80S (right arrow), and ribosomal absorbance peaks (asterisks). An equal aliquot of purified RNA from each fraction was run on a 1%agarose gel to verify the sedimentation of rRNAs (18S and 28S) in the deeper sucrose fractions. D, quantitative RT-PCR fold changes of select genes from multiple Wnt/iR1 tumors over multiple Wnt-1 tumors through all nine fractions of the sucrose gradient. Fractions were divided into soluble, nonpolysome bound (fractions 1–4), and polysome bound (fractions 5–9) and compared (Supplementary Fig. S6). cMyc ($n = 5$): ‡, $P < 0.0005$; survivin ($n = 3$): ‡, $P < 0.02$; cyclin D ($n = 4$): ‡, $P < 0.003$. Whole-cell (WC) mRNA was also analyzed. cMyc, survivin, and cyclin D: †, $P > 0.05$, normalized to 18S. Columns, mean; bars, SE.

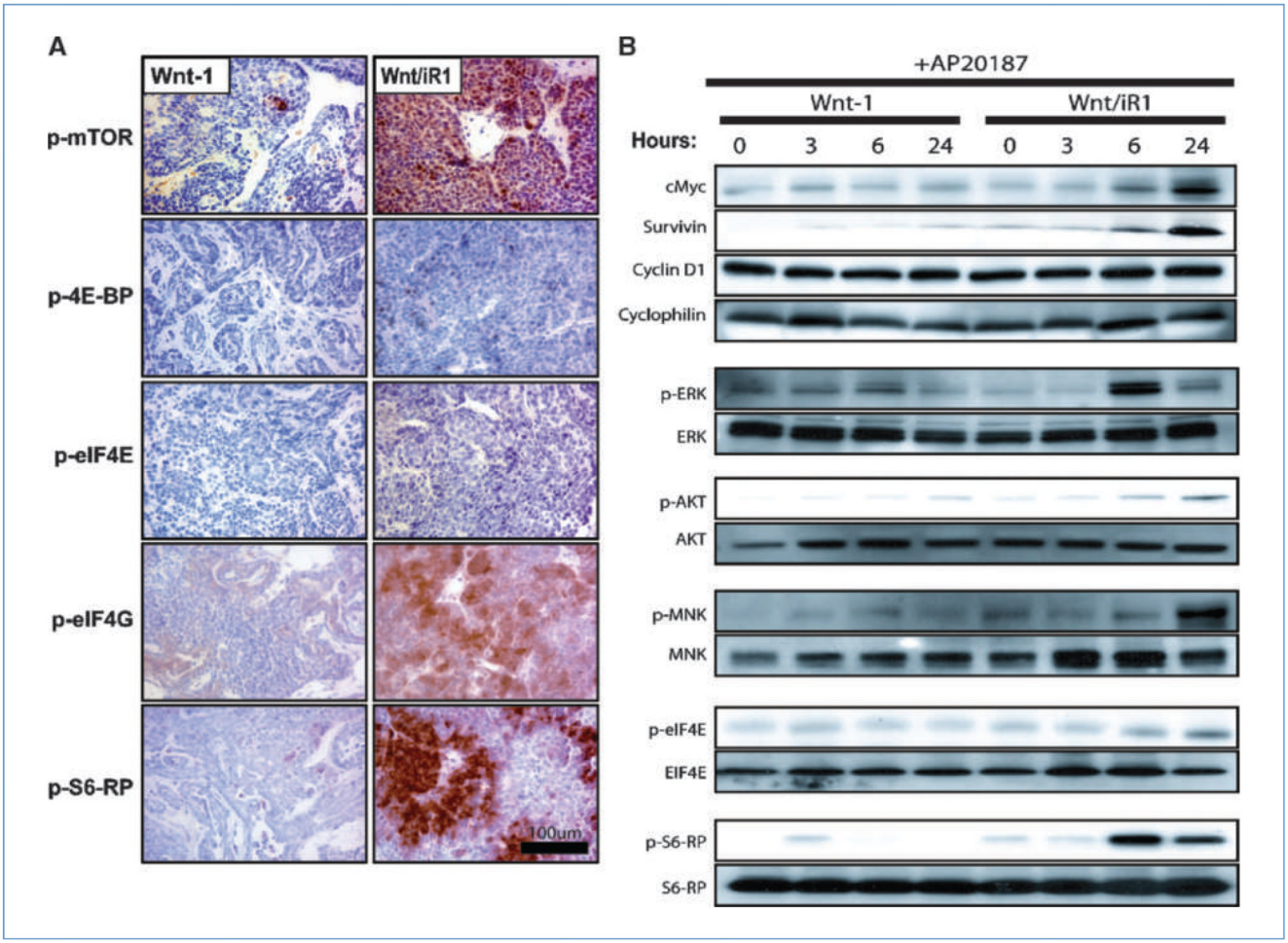

Figure 5.

iFGFR1 dimerization leads to increased phosphorylation of critical translational regulators. A, immunohistochemistry of several critical translational pathway regulators. At least two to three tumors were analyzed per mouse/stain. B, immunoblot analysis of Wnt-1 and Wnt/iR1 mammary gland lysates 0, 3, 6, and 24 h following dimerizer. Protein levels of cMyc, survivin, and cyclin D1 were analyzed as well as phospho-specific phospho-ERK, phospho-MNK, phospho-eIF4E, phospho-AKT, and phospho–S6-RP. Enhanced cMyc and survivin were observed within the 6- to 24-h time period in at least two to three sets of animals. Enhanced phosphorylation of ERK and AKT was observed in at least two to three sets of animals within the 6- to 24-h time period. Phosphorylation of MNK, eIF4E, and S6-RP was observed in one set of four animals per tumor type from 0 to 24 h following injection of dimerizer. Cyclophilin A, total ERK, AKT, MNK, eIF4E, and S6-RP were used as loading controls.

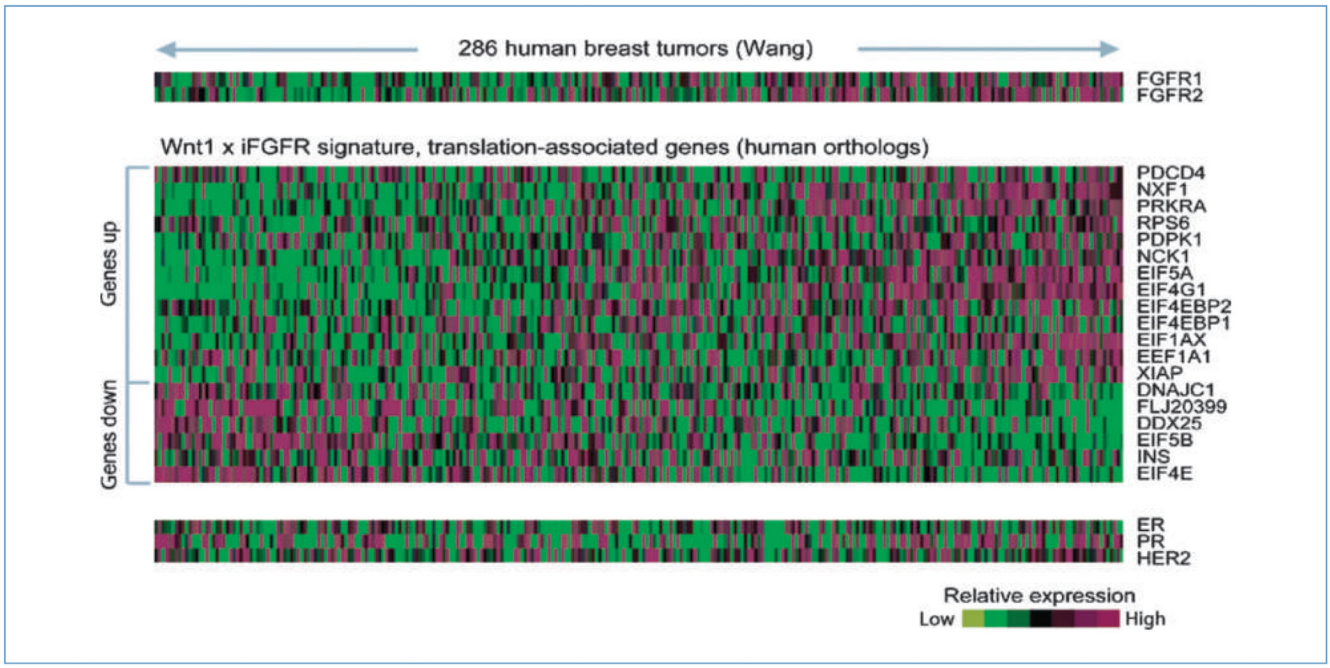

Figure 6.

High FGFR expression correlates with the protein translational gene signature in human breast cancer. Heat map comparing FGFR1 and FGFR2 expression levels with protein translational gene signature from Fig. 3 within the Wang data set (37). FGFR1: $P = 4E{-}08$, FGFR2: $P = 3E{-}11$.

Table 1

List of five data sets with correlation significance values

Data set	No. tumors	FGFR1		FGFR2	
		***R* value**	***P***	**R value**	***P***
Wang (37)	286	0.31	4E−08	0.37	3E−11
van de Vijver (38)	295	0.03	0.31	0.25	5E−06
Desmedt (41)	198	0.23	0.0007	0.10	0.09
Hoadley (40)	248	0.24	5E−05	0.08	0.12
Loi (39)	414	0.15	0.0012	0.13	0.004

Cancer Res. Author manuscript; available in PMC 2011 June 15.